Sheltered load in fungal mating-type chromosomes revealed by fitness experiments

Lou Guyot[1,2], Elizabeth Chahine[1], Christophe Lalanne[3], Fanny E. Hartmann[1*], Tatiana Giraud[1*]

1 Ecologie, Systematique et Evolution, CNRS, Universite Paris-Saclay, AgroParisTech, Gif-sur-Yvette, France

2 Master de Biologie, Ecole Normale Supérieure de Lyon, Universite Claude Bernard Lyon 1, Universite de Lyon, 69342 Lyon Cedex 07, France

3 Laboratoire Interdisciplinaire des Energies de Demain, Université Paris Cité, Paris, France

*FEH and TG are joint senior authors on this work.

Keywords: overdominance, heterozygous advantage, mutational load, self-incompatibility locus, sex chromosome, fungi, mating-type locus

Corresponding author: tatiana.giraud@universite-paris-saclay.fr

Abstract

Sex chromosomes and mating-type chromosomes can carry large regions with suppressed recombination. In these non-recombining regions, recessive deleterious mutations are expected to occur, as i) they are predicted to accumulate as a result of lower efficacy of selection, and ii) they may even pre-exist and drive the evolution of recombination suppression. Multiple genomic analyses have indirectly inferred the presence of deleterious mutations in sex and mating-type chromosomes, but direct experimental evidence remains scarce. Here, we performed fitness assays in fungi with megabase-large and young non-recombining regions around the mating-type locus, using the *Schizothecium tetrasporum* and *Podospora anserina* species complexes, to test whether heterokaryons (diploid-like, heterozygous at the mating-type locus) exhibited a fitness advantage over homokaryons (haploid-like, with a single mating-type allele), in terms of spore germination dynamics or mycelium growth speed, under different conditions of light and temperature. We found a faster growth of heterokaryons compared to one of the homokaryons for *P. anserina* at 18°C, for *S. tetrasporum* and *S. tritetrasporum* at 22°C under light, and also at 22°C in the dark for *S. tetrasporum*. These findings suggest the presence of a sheltered load, i.e. recessive deleterious mutations at the heterozygous state in or near non-recombining regions, as these species are highly homozygous otherwise. Leveraging on the experimental assets of fungi, allowing cultivating separately haploid-like and diploid-like life stages, our experiments provided one of the rare direct experimental evidence of sheltered load around mating-compatibility loci, which is crucial for our understanding of sex-related chromosome evolution.

Introduction

Even in sexual species, genomes can display large non-recombining regions (Wright et al., 2016, Schwander et al., 2014, Bergero & Charlesworth, 2009). Such non-recombining regions are particularly frequent around sex-determining loci and mating-type loci (Charlesworth, 2017, Wright et al., 2016, Ma & Veltsos, 2021, Hartmann et al., 2021b, Jay et al., 2024, Nicolas et al., 2004, Branco et al., 2017, Branco et al., 2018, Papadopulos et al., 2015, Bachtrog, 2005, Bachtrog, 2013, Hallast et al., 2023). Deprived of recombination, these genomic regions experience a reduced efficacy of selection (Felsenstein, 1974, Muller, 1932, Hill & Robertson, 1966, Rice & Chippindale, 2001, Otto, 2009, Colegrave, 2002). As a consequence, it has been theoretically suggested that non-recombining regions are bound to degenerate (Smith & Haigh, 2009, Muller, 1932, Hill & Robertson, 1966, Fisher, 1930), i.e., to accumulate recessive deleterious mutations following recombination suppression. In addition, theoretical models have shown that recessive deleterious alleles can be maintained at the margin of self-incompatibility loci in linkage disequilibrium with it (Tezenas et al., 2023, Antonovics & Abrams, 2004, Glémin et al., 2001, Uyenoyama, 2005). It has even been suggested that the presence of recessive deleterious mutations around permanently heterozygous alleles (e.g. a mating-type allele or a Y-like sex-determining allele) might be the cause of the selection of recombination suppression, and not only a consequence (e.g., for sheltering recessive deleterious mutations around a permanently heterozygous allele; (Branco et al., 2017, Jay et al., 2021, Jay et al., 2024, Lenormand & Roze, 2022)). In both cases, one expects recessive deleterious mutations to occur in non-recombining regions around sex-determining or mating-type determining alleles. Such recessive deleterious mutations

associated with a permanently heterozygous allele constitute a sheltered load, as they are also heterozygous and therefore not exposed to selection.

The presence of deleterious mutations in non-recombining mating-type and sex chromosomes has been indirectly inferred through genomic analyses, that have for example revealed gene disruptions, gene losses, non-synonymous substitutions, transposable element accumulation and chromosomal rearrangements (Carpentier et al., 2022, Vittorelli et al., 2023, Duhamel et al., 2023, Bachtrog, 2005, Bachtrog, 2013, Charlesworth & Charlesworth, 2000, Fontanillas et al., 2015, Hough et al., 2014, Papadopulos et al., 2015, Whittle et al., 2011). However, there has been little direct evidence for the existence of such sheltered load through experimental fitness assays so far. To perform such experiments, one indeed needs to compare fitness between a haploid phase or a homozygous state to the heterozygous diploid state, i.e. between situations where mutations are exposed to selection to situations where deleterious mutations are sheltered. Such situations can be found in autosomal supergenes, i.e., non-recombining regions in autosomes governing adaptive and complex phenotypes (Schwander et al., 2014). Using autosomal supergenes that can be homozygous, the existence of sheltered load could be demonstrated in a few cases (Jay et al., 2021). A few balanced haplo-lethal systems even exist, in which recessive deleterious mutations are lethal at the homozygous state in non-recombining supergenes (Wielstra, 2020, Hill et al., 2023). However, in the majority of organisms with non-recombining regions on sex-related chromosomes, haploid or homozygous states do not occur in the life cycle and cannot be generated in these non-recombining regions. The rare exceptions include self-incompatibility loci in plants that can be rendered homozygous under certain conditions. Sheltered load was found associated with the most dominant self-incompatibility allele in *Arabidopsis halleri*, at several stages of the life cycle, using elevated CO_2 concentrations for disrupting self-

incompatibility (Stone, 2004, Llaurens et al., 2009). Sheltered load has also been experimentally shown around the self-incompatibility locus in the plant *Solanum carolinense* by using life stages where self-incompatibility is less strong to obtain homozygous plants at the self-incompatibility locus (Mena-Alí et al., 2009). However, in the case of self-incompatibility loci, regions without recombination are generally small, restricted to the self-incompatibility locus (Goubet et al., 2012), and the existence of multiple alleles may render unlikely the mechanism driving recombination suppression for sheltering pre-existing load (Jay et al., 2022).

Fungi can be highly tractable models for investigating the existence of a sheltered load in sex-related chromosomes. Indeed, there can be recombination suppression around their mating-type loci in species with a long heterokaryotic (diploid-like) phase, i.e., with nuclei of opposite mating types per cell, but unfused, which is functionally similar to a diploid stage (Branco et al., 2017, Branco et al., 2018, Hartmann et al., 2021b, Fraser et al., 2004, Jay et al., 2024, Grognet et al., 2014, Bakkeren & Kronstad, 1994, Menkis et al., 2008, Vittorelli et al., 2023). In addition, many fungi display only two mating types (Billiard et al., 2011), and recombination suppression around the mating-type locus has been detected only in those (Jay et al., 2024). Genomic footprints of degeneration have been found in these non-recombining regions, in the form of gene losses, transposable element accumulation, non-synonymous substitutions and non-optimal codon usage and expression (Carpentier et al., 2022, Vittorelli et al., 2023, Duhamel et al., 2023, Fontanillas et al., 2015, Whittle et al., 2011). In addition, the life cycle of many fungi allows fitness comparison between haploid and heterokaryotic stages (Grognet et al., 2014).

Mating types in fungi do not prevent selfing, as mating compatibility is controlled at the haploid stage (Billiard et al., 2012, Giraud et al., 2008). As a matter of fact, the fungal lineages with recombination suppression around their mating-type loci most often undergo regular automixis i.e. intra-tetrad selfing (Billiard et al., 2012, Giraud et al., 2008, Hood & Antonovics, 2000, Zakharov, 2005, Zakharov, 2023, Grognet et al., 2014, Jay et al., 2024, Vittorelli et al., 2023), so that their genomes are highly homozygous in their extended diploid-like phase, except in the non-recombining region around the mating type locus (Branco et al., 2017, Branco et al., 2018, Hartmann et al., 2021a, Vittorelli et al., 2023). Such life cycles in fungi are called pseudo-homothallic, with the production of self-fertile heterokaryotic spores, encompassing two nuclei of opposite mating types originating from a single tetrad after meiosis, thus germinating as a self-fertile heterokaryon and undergoing mostly automixis. Self-sterile spores with a single mating type, germinating as homokaryotic mycelia, can also generally be produced in laboratory conditions, although their importance in nature is unknown. With such life cycles, experiments can be set up for comparing the fitness between homokaryons (i.e. with a single type of nuclei per cell) and heterokaryons (i.e. with nuclei of opposite mating types in each cell) in order to study the heterozygous advantage in the region around the mating-type locus (Fig 1A). Indeed, in natural heterokaryotic strains, that are typically highly homozygous genome-wide except around the mating-type locus, because of high selfing rates, any variability in fitness between homokaryotic and heterokaryotic stages should mainly be due to heterozygous recessive deleterious mutations present in the non-recombining region around the mating-type locus and possibly in its flanking region due to linkage disequilibrium (Branco et al., 2017, Tezenas et al., 2023, Glémin et al., 2001). Some recessive lethal alleles have been revealed in anther-smut fungi of the *Microbotryum* genus, by the lack of growth of haploids of one mating type in some populations or species (Hood & Antonovics, 2000, Thomas et al., 2003, Oudemans

et al., 1998). Balanced lethals linked to the mating-type locus have also been shown in the fungal-like oomycete *Phytophthora infestans* (Judelson et al., 1995).

We studied here five species of two phylogenetically distant fungal species complex within the Sordariales order of Ascomycota: *Schizothecium tetrasporum* and *Schizothecium tritetraporum*, belonging to the *Schizothecium tetraporum* species complex (Vittorelli et al., 2023), and *Podospora anserina*, *Podospora comata* and *Podospora pauciseta*, belonging to the *Podospora anserina* species complex (Grognet et al., 2014, Hartmann et al., 2021a, Boucher et al., 2017). These species are coprophilous, saprophyte or endophyte, and can be found in herbivore faeces and soil (Silar, 2020). These fungi are excellent biological models to investigate the presence of a sheltered load around their mating-type locus, displaying only two mating-type alleles (*MAT1-1* and *MAT1-2*, also called *mat*- and *mat*+, respectively). Indeed, these fungi display recombination suppression around their mating-type loci, as shown by progeny segregation and nucleotide divergence analyses (Grognet et al., 2014, Hartmann et al., 2021a, Vittorelli et al., 2023), and are pseudo-homothallic, i.e. with their main life cycle phase being heterokaryotic (Grognet et al., 2014, Vittorelli et al., 2023), so that sheltered load can be expected. Recombination suppression around the mating-type locus spans approximately 1 Mb in the *S. tetrasporum* and *P. anserina* species complexes and has been suggested to be quite recent, as indicated by the low divergence between mating types and the lack of trans-specific polymorphism (Vittorelli et al., 2023, Grognet et al., 2014, Hartmann et al., 2021a). Indirect evidence of sheltered load has been reported by genomic analyses in their non-recombining regions, in particular a few gene losses or disruptions (Vittorelli et al., 2023, Grognet et al., 2014). Furthermore, recombination suppression around the mating-type locus represents convergent events between the *S. tetrasporum* and *P. anserina* species complexes, that diverged over 150 million years ago, which provides

168 independent events of recombination suppression to study. Even within each of these two
169 species complexes, recombination suppression has likely evolved independently in the
170 various species, as suggested by the lack of trans-specific polymorphism and sizes of the non-
171 recombining regions (Hartmann et al., 2021a). In addition, natural strains are highly
172 homozygous genome-wide, except around the mating-type locus (Vittorelli et al., 2023,
173 Grognet et al., 2014, Hartmann et al., 2021a). Another asset of these models is that one can
174 cultivate *in vitro* homokaryotic and heterokaryotic mycelia (Figs 1A and 1B). In addition,
175 while most ascospores are heterokaryotic, homokaryotic spores are sometimes produced and
176 are easily distinguishable based on their smaller size (Vittorelli et al., 2023, Silar, 2020) (Fig
177 1C). In *S. tetrasporum* and *P. anserina*, previous experiments on a single strain did not detect
178 any heterokaryon advantage (Grognet et al., 2014, Vittorelli et al., 2023). However, a
179 difference in mycelium growth speed between *MAT1-1* and *MAT1-2* homokaryons has been
180 reported in *P. anserina*, but again using a single strain, when grown at stressful temperature
181 (37°C; (Contamine et al., 2004)). *Podospora anserina* indeed does not tolerate high
182 temperatures (Silar, 2020). Light is also an important regulator of diverse physiological
183 processes in *P. anserina* (Shen et al., 2022). Studying multiple strains is essential in
184 evolutionary biology, as the effects of deleterious mutations can depend on epistatic effects
185 and/or be present in only some individuals in populations, while still having important
186 population effects.
187
188 Here, we thus conducted assays using different fitness proxies on a dozen strains of each of *S.*
189 *tetrasporum*, *S. tritetrasporum* and *P. anserina*, by comparing heterokaryons and
190 homokaryons (Fig 1), in terms of mycelium growth speed under light or dark, at different
191 temperatures, and in terms of spore germination dynamics. We also ran exploratory fitness
192 experiments on small numbers of strains on *P. comata* and *P. pauciseta*. Our analyses reveal

a fitness advantage of heterokaryons over one of the homokaryons (either *MAT1-1* or *MAT1-2*) in at least one tested condition for *S. tetrasporum*, *S. tritetrasporum* and *P. anserina*, indicating the likely existence of a sheltered load in the non-recombining region present around the mating-type locus and/or in its flanking region. In contrast, we found a faster growth of one of the homokaryons compared to heterokaryons at 37°C in *P. pauciseta* and no difference in *P. comata*, but small numbers of strains were available for these species.

Material and Methods

Strains

The information on the strains is given in Supplementary Table 1 (strain ID, species, collection, year, substrate and geographic region of collection). We used 10 heterokaryotic strains of *S. tetrasporum* and 13 heterokaryotic strains of *S. tritetrasporum* stored at -80°C. We obtained homokaryotic mycelium of the *MAT1-1* and *MAT1-2* mating types for each heterokaryotic strain as described previously (Vittorelli et al., 2023, Silar, 2020). Briefly, a plug of heterokaryotic mycelium (5 mm^3) was grown for each strain on a V8 medium Petri dish for two to three weeks until perithecia formation. Then, agar Petri dishes were added on the top, upside down, to collect projected spores (Silar, 2020). Homokaryotic spores were then isolated, identified by their smaller size compared to heterokaryotic spores, and grown on Petri dishes with G medium (Silar, 2020) (Fig 1C). These Petri dishes were subjected to a heat shock (30 minutes at 65°C) to induce spore germination. After a few days of growth, mycelia were transferred on M2 medium for growth. The mating-type allele of homokaryotic mycelium grown from those spores was identified by PCR. For this goal, DNA was extracted using Chelex and the mating-type allele (*MAT-1-1* or *MAT1-2*) was determined using the PCR conditions described previously (Vittorelli et al., 2023) and the following primer pairs:

MAT-1-2 5''GAGGGTGCGAGTCGTGAT'3' and 3''CCAGCCACACGAAAATCC'5'; *MAT-1-1* 5''GATCGGATTCGCTCCAGA'3' and 3''CGACCGTTGGAAATGACC'5'.

We also used 17 heterokaryotic strains of *Podospora anserina*, one heterokaryotic strain of *P. comata* and three heterokaryotic strains of *P. pauciseta* (Supplementary Table 1), with *MAT1-1* and *MAT1-2* homokaryotic mycelium stored at -80°C.

Inoculum preparation

Prior to each experiment, *MAT-1-1* and *MAT1-2* homokaryotic mycelia of the studied heterokaryotic strains were grown on M2 medium (Silar, 2020) for about 7 to 15 days at 27°C, 50% humidity and light and then stored at 4°C for a few days until the beginning of the experiments. On the day of inoculation, fresh inoculum was prepared. Mycelium square plugs of the two mating types for each strain were crushed separately (to form homokaryotic mycelium solutions) and also together (to generate heterokaryotic mycelium solutions; (Silar, 2020, Vittorelli et al., 2023)), with 200 µL of sterile water for *S. tritetrasporum* and *S. tetrasporum* and 150 µL of sterile water for the other species, using a TissueLyser at 30 Hz for 20 to 30 min.

Growth speed

Spots of 20 µL of the obtained solutions for homokaryotic mycelium *MAT1-1*, homokaryotic mycelium *MAT1-2* or heterokaryotic mycelium were deposited on Petri dishes with M2 medium (Silar, 2020), with three replicates per strain and condition. One central spot was deposited per Petri dish, corresponding to a replicate. For *S. tritetrasporum*, two batches were performed at different times. Plates were incubated at the conditions of temperature and light exposure detailed in Table 1. Pictures of the plates were taken on two days (see details of the days for each species in Table 1). As the mycelium limits of *P. anserina*, *P. comata* and *P.*

pauciseta were not always clearly distinguishable on pictures, the contour of the mycelial colony was drawn with a marker pen under the Petri dish before taking the picture. Diameters of mycelia were measured using ImageJ 1.54g (Schneider et al., 2012), and the growth speed was computed as the difference in diameter between the two days divided by the number of growth days. We measured one diameter per Petri dish, at the same location for the different time points, using as a reference the label that had been put under the Petri dishes before growth. Some Petri dishes were excluded from the analysis when contamination, dryness or satellite colonies occurred (see Table S2 with raw data).

PCRs were performed on heterokaryotic mycelia 14 days post-inoculation for all *S. tritetrasporum* strains in the two experiment batches to check whether they remained heterokaryotic. Nine plugs (5 mm^3) were sampled in each Petri dish from the inner to the outer of the mycelium ring. DNA was extracted using Chelex and the mating-type allele (*MAT-1-1*, *MAT1-2* or both) was determined using the PCR conditions and the primer pairs described above. When only a faint band appeared for one of the two mating types, the PCR was re-run to check the presence of the second band. Some PCRs did not yield any band at all, for neither mating type, and the corresponding plugs were excluded from the analysis on heterokaryon persistence (see Table S2 with raw data).

Germination dynamics

For the 10 heterokaryotic strains of *S. tetrasporum*, three spots of 20 µL of heterokaryotic mycelium solution were deposited on a single Petri dish with V8 medium (Vittorelli et al., 2023) and incubated at 22°C until perithecia formation (about 15 days). PSN881A and PSN779 strains did not produce any perithecia and were excluded from the analysis. Agar Petri dishes were added on the top, upside down, to collect projected spores (Vittorelli et al.,

2023). We isolated 10 large spores and 10 small spores per heterokaryotic strain, which were deposited on a Petri dish with G medium (Silar, 2020), allowing germination (two batches per strain). Small spores are homokaryotic, while large spores are heterokaryotic at the mating-type locus with a 90% probability, as estimated in (Vittorelli et al., 2023) based on genotyping of the germinated mycelium, which is a minimum estimate, as the mycelium could also have lost a nucleus during growth before genotyping. These Petri dishes were foiled with aluminium paper, subjected to a heat shock of 30 min at 65°C and incubated at 27°C to induce germination (Silar, 2020). Germinated spores were counted on days 2, 3 and 7 to analyse the germination dynamics of small and large spores, i.e. the rates of germination over time (Table 1). A few spores were excluded from the analysis when there was contamination or two spores were observed germinating instead of one (see Table S3 with raw data).

Graphical summaries and statistical analyses

Statistical analyses and graphic displays were performed using R software v 4.3.2 (R Core Team, 2023). For the growth experiment analyses, a linear mixed-effect model was used for all tested conditions for *S. tritetrasporum*, *S. tetrasporum*, *P. anserina* and *P. pauciseta*, explaining growth speed using the nuclear status (i.e. heterokaryotic, *MAT1-1* or *MAT1-2* homokaryotic) as a fixed effect and the strain ID as a random effect. In *S. tritetrasporum*, a random effect for the batch was added. For *P. comata*, a single strain was used; a linear model was therefore used with growth speed as the outcome and nuclear status (i.e. heterokaryotic, *MAT1-1* or *MAT1-2* homokaryotic) as a predictor. For the germination experiment analysis in *S. tetrasporum*, a generalised linear mixed-effect model with a binomial distribution was used, modelling germination rate as a linear combination of day (as a continuous predictor) and spore size class (large or small) treated as fixed effects, and strain

ID and batch as random effects. A statistical significance level of 5% was considered for all statistical tests. For linear and linear mixed-effect models, predictions with standard deviations are represented and p-values from Student t-tests are reported (with Satterthwaite correction for the linear mixed-effect models), with default contrast coding (i.e, for a three-level categorical predictor, only two regression coefficients are tested, excluding the reference category, here set to be the heterokaryotic nuclear status, which is subsumed in the intercept term). Omnibus tests for the overall significance of statistical models were based on F-tests, with Satterthwaite's approximation for the degrees of freedom (DoF) in the case of mixed-effects models, where the first and second DoFs correspond to the effect and the residuals of the model, respectively. When considering a statistical model with a single categorical predictor with k levels, this test can be seen as a joint test of all k levels (instead of individual t-tests for all k-1 levels, excluding the reference level). In the case of the generalised linear mixed-effects model, predictions with standard deviation obtained with the Laplace approximation are represented and p-values from χ2-tests are reported. The linearity of the response and predictor relationship and the Gaussian distribution of the residuals in all models (including random effects intercept and slope in the case of random-effects models) were assessed visually using R built-in facilities (fitted vs. residual values plot and QQ-plot, respectively).

Results

To investigate the presence of sheltered load in the non-recombining regions around the mating-type locus, or at their margin, in *S. tetrasporum*, *S. tritetrasporum* and *P. anserina*, experiments were performed in each species to compare the fitness of heterokaryons to that

of homokaryons using strains as biological replicates (10, 13 and 17 strains, respectively; Table S1; Fig 1). Exploratory fitness analyses were run on smaller numbers of strains in *P. comata* and *P. pauciseta* (one and three strains, respectively). For *S. tetrasporum* and *S. tritetrasporum*, we used as fitness proxies the mycelium growth speed under light at 22°C between day 6 and day 14. In addition, we used as fitness proxies for *S. tetrasporum* the mycelium growth speed under dark at 22°C and assessed the spore germination dynamics between day 2 and day 7. For *P. anserina*, *P. comata* and *P. pauciseta*, we measured mycelium growth speed between day 2 and day 6 under light at 18°C and 37°C. These conditions were chosen for each species based on preliminary experiments or previous knowledge on the different species to use more or less stressful conditions. Table S2 gives the raw measures for the growth experiment for which 5% of plates have been excluded on average per analysis due to the presence of satellite colonies, contaminants or dryness. Table S3 gives the raw measures for the germination experiment, for which two out of the 10 strains of *S. tetrasporum* were excluded due to lack of perithecia and less than 1% of the spores were excluded, due to contamination or the germination of two spores, meaning that two spores had been deposited instead of one.

In *S. tritetrasporum*, heterokaryons grew significantly faster than homokaryons *MAT1-1* under light at 22°C by 5.6% (Figs 2 and S1; $F(2, 192.3)=7.9683$, p-value=0.0005). In *S. tetrasporum*, heterokaryons also grew significantly faster than homokaryons *MAT1-1* under light at 22°C by 5.5% (Figs 3A and S2A; $F(2, 70.2)=4.5497$, p-value=0.0139), while heterokaryons grew significantly faster than homokaryons *MAT1-2* in the dark at 22°C by 4.0% (Fig 3B and S2B; $F(2, 67.2)=5.9887$, p-value= 0.0040).

Given that some level of nuclear loss of one mating type has been reported to occur during heterokaryotic mycelium growth in the *S. tetrasporum* species complex (Vittorelli et al.,

2023), we used PCR to test whether and to what extent such a phenomenon occurred in our *S. tritetraporum* heterokaryotic mycelia used for growth experiments, by genotyping the mating-type locus for nine plugs per Petri dish. We found that mycelia had remained mostly heterokaryotic (Figs S1 and S3).

In *P. anserina* under light conditions, heterokaryons grew significantly faster than homokaryons *MAT1-2* at 18°C, by 8.1% (Figs 4A and S4A; $F(2, 128.4)=5.7881$, p-value=0.0039). The tendency was similar at 37°C but the difference was not significant (Figs 4B and S4B; $F(2, 133.0)=1.4409$, p-value=0.2404).

We found a similar tendency in *P. pauciseta* at 18°C, but not significant (Figs 5A and S5A; $F(2, 22)=1.4184$, p-value=0.2634). In contrast, we found a significantly slower growth of heterokaryons compared to *MAT1-1* homokaryons at 37°C in *P. pauciseta*, by 27.6% (Fig 5B and S5B; $F(2, 21)=4.0481$, p-value=0.0326). In *P. comata*, both homokaryons also seemed to grow faster than heterokaryons at 18°C (Figs 5C and S5D; $F(2, 6)=2.348$, p-value=0.1765) and 37°C (Figs 5D and S5D; $F(2, 6)=1.1963$, p-value=0.3654), although it was not significant. However, we had only three and one strains for these species, respectively, so little conclusion can be inferred from these species at the population scale. Note that *P. comata* grew very little at 37°C, indicating that it represents a too stressful condition for this species.

The comparison of the germination dynamics of small spores (i.e. homokaryotic spores) versus large spores (i.e. mainly heterokaryotic spores; (Vittorelli et al., 2023)) in *S. tetrasporum* did not reveal any evidence of heterozygous advantage (Figs 6 and S6).

Discussion

Likely presence of recessive deleterious mutations around the mating-type locus

Our fitness assay showed that heterokaryons were fitter than at least one homokaryon under light at 18°C in *P. anserina* and at 22°C in *S. tetrasporum* and *S. tritetrasporum*, and also at 22°C in the dark in *S. tetrasporum*, suggesting heterozygote advantage. Such results are most likely due to the presence of recessive deleterious mutations in the non-recombining region around the mating-type locus, being associated to a single mating-type allele, and/or in linkage disequilibrium with the mating-type locus in the margin of the non-recombining region, these mutations being expressed at the homokaryotic state but sheltered at the heterokaryotic state**.** Our findings thus suggest the existence of a sheltered load near the mating-type locus in the studied fungi with a sample size of at least 10 strains.

Our study is one of the very rare experimental studies showing the existence of a sheltered load for sex-related chromosomes. Only a few studies could investigate a sheltered load so far, around self-incompatibility loci in plants (Stone, 2004, Llaurens et al., 2009) as this is one of the rare systems where mating-type loci can be rendered homozygous. To investigate the presence of a sheltered load, we leveraged on another unique biological system, pseudo-homothallic fungi, whose life cycle allows fitness comparison between individuals in which mutations around the mating-type locus are sheltered versus exposed to selection, while the rest of the genome is exposed to selection, being highly homozygous due to high selfing rates in nature. Our study thus provides unique experimental evidence of a sheltered load around mating-type loci, i.e. of heterozygous recessive deleterious mutations in the non-recombining region, in three fungal species with independent events of recombination suppression.

Previous evidence in fungi include haplo-lethal alleles linked to mating types in anther-smut fungi and oomycetes, in which one or the two mating types fail to grow at the haploid stage or cause a segregation bias in progenies (Hood & Antonovics, 2000, Thomas et al., 2003, Oudemans et al., 1998, Judelson et al., 1995), but the non-recombining regions were much older in these cases. Here, we reveal the existence of a sheltered load in very young non-recombining regions (Hartmann et al., 2021a, Vittorelli et al., 2023, Grognet et al., 2014). Recessive deleterious mutations have also been experimentally shown to occur in a few autosomal supergenes (Jay et al., 2021, Wielstra, 2020, Hill et al., 2023). Altogether, such direct experimental evidence of sheltered load is important for understanding the evolution of non-recombining regions.

The lack of significant heterozygote advantage detected in certain conditions might be due to the genes with putative deleterious alleles having little role under these conditions, the weak effect of the mutations, and/or the low number of mutations. In all three fungal species with a sample size of at least 10 strains, the heterokaryons indeed grew faster than at least one homokaryon in at least one condition, and showed similar tendencies across all conditions. The growth advantage was around 5%, which may constitute a non-negligible advantage to colonise short-lined habitats such as faeces. The spore germination dynamics in contrast did not seem different between small and large spores. Heterozygous advantage need not be expressed in all stages of the life cycle or in all strains to have a significant fitness effect in natural populations: even if the heterozygous advantage only holds at some temperature and during growth (and not during germination), it may incur non-negligible fitness advantage if these conditions are frequent enough in natural populations.

No significant heterozygote advantage was detected in *P. comata* and we even found a heterozygote disadvantage in *P. pauciseta* at 37°C, but we only used one or three strains for these species as preliminary experiments. Such a heterozygote disadvantage could be due to negative epistasis or outbreeding depression; indeed, although these species are highly selfing, some rare events of outcrossing do occur (Hartmann et al., 2021a). However, further natural strains would need to be analysed to draw conclusive inferences. In *S. tetrasporum* and *P. anserina* for example, experiments on a single strain did not detect any heterokaryon advantage in previous studies (Grognet et al., 2014, Vittorelli et al., 2023), while it was revealed here with a dozen strains. For *P. pauciseta* at 18°C, the heterokaryon seemed to grow faster than homokaryons, and this condition may be worth exploring using additional strains and conditions. Indeed, in previous studies in which a single strain of *P. anserina* had been studied (Grognet et al., 2014), a significant difference had been found at 37°C between the two homokaryons but not at 22°C (Grognet et al., 2014, Contamine et al., 2004). Here, *P. comata* did not grow much at 37°C, and it may be worth exploring lower but still stressful temperatures.

Few other studies have compared fitness proxies between homokaryons and heterokaryons in fungi. In three lineages of *Neurospora tetrasperma*, another Sordariales fungus with recombination suppression around its mating-type locus, fitness estimates have been computed comparing heterokaryons with different nuclei ratios and also compared to homokaryons, using as a proxy the quantity of asexual haploid spores (conidia) produced by mycelia. In each lineage, one mating type produced more spores than the other mating types, and heterokaryons appeared intermediate (Meunier et al., 2018). This suggests codominance for the alleles controlling spore quantity, and no sheltered load affecting this trait. Few strains have however been analysed in this study (Meunier et al., 2018).

436

437 **Sheltered load originating post- or pre-recombination suppression and models of sex**
438 **chromosome evolution**

439 Our results on the three species with at least ten strains, i.e., *S. tetrasporum*, *S. tritetrasporum*
440 and *P. anserina*, support the prediction that recessive deleterious mutations occur in the non-
441 recombining regions around mating-type loci and/or at its margin. However, our
442 experimental setting does not allow distinguishing whether the load occurred before or after
443 recombination suppression. Indeed, recessive deleterious mutations might have accumulated
444 as a consequence of recombination suppression (Smith & Haigh, 2009, Muller, 1932, Hill &
445 Robertson, 1966, Fisher, 1930) and/or before recombination suppression (Tezenas et al.,
446 2023, Antonovics & Abrams, 2004, Glémin et al., 2001, Uyenoyama, 2005), and then even
447 possibly driving the evolution of recombination suppression (Jay et al., 2024, Jay et al., 2022,
448 Branco et al., 2017). The young age of the recombination suppression in these species gives
449 plausibility to an origin of the deleterious mutations before recombination suppression.

450

451 We found significant differences in terms of growth speed, in the species with at least ten
452 strains, i.e., *S. tetrasporum*, *S. tritetrasporum* and *P. anserina*, between heterokaryons and a
453 single one of homokaryons. In *S. tetrasporum*, the homokaryon displaying a disadvantage
454 was not the same in the different conditions, suggesting the existence of deleterious mutations
455 in both haplotypes, but different ones. This altogether may be because of stochastic
456 accumulation of recessive deleterious mutations following recombination suppression in the
457 non-recombining region or at its margin, with specific mutations affecting by chance one
458 mating type and not the alternative one. It may also be because recombination suppression
459 was actually due to selection for a non-recombining fragment with fewer deleterious
460 mutations than average in the population (Jay et al., 2021, Jay et al., 2024); in this case, the

corresponding homokaryon would be expected to initially carry a particularly light load compared to the alternative mating type.

We found relatively weak differences in fitness (ca. 5% differences in mycelium growth speed) and the heterozygous advantage was not detected in all traits, which may be explained by the young age of the recombination suppression and/or by a non-negligible haploid phase that would purge to some extent recessive mutations with large detrimental effect**.** Indeed, although rare, some homokaryotic spores are produced in these fungi: in *S. tetrasporum*, 2% to 10% of asci with small (i.e. homokaryotic) spores have been reported (Raju & Perkins, 1994, Vittorelli et al., 2023). In *P. anserina*, 5% of spores are homokaryotic (Ament-Velásquez & Vogan, 2022). The loss of nuclei of one mating type during mycelium growth in *Schizothecium* fungi may also expose recessive deleterious mutations to selection. Therefore, because of the young age of recombination suppression and the existence of a non-negligible haploid phase, even if limited, we do not expect a high load in the non-recombining region. Nevertheless, we documented the existence of a sheltered load, which may have pre-existed and/or accumulated following recombination suppression.

Alternative hypotheses to sheltered load

There may however be alternative hypotheses explaining the higher fitness of heterokaryons. Although the species used mainly reproduce by selfing and most strains display genome-wide homozygosity(Grognet et al., 2014, Hartmann et al., 2021a, Vittorelli et al., 2023), some rare events of outcrossing can generate short tracks of heterozygosity in genomic regions far from the mating-type locus, which could also have provided a heterozygote advantage in *S. tetrasporum*, *S. tritetrasporum* and/or *P. anserina.* It could also be due to a heterozygous advantage not related to deleterious mutations, although such advantages are rare in nature

and mostly related to host-parasite interactions (Gemmell & Slate, 2006), and therefore unlikely in our experimental setting.

The heterokaryon advantage detected may also be due, in principle, to a ploidy advantage, for example, related to gene expression dosage, which may be expected to be twice as high in heterokaryons as in homokaryons. It is not clear, however, whether heterokaryons have twice as many nuclei as homokaryons, as there are multiple nuclei per cell in both types of mycelia (Sylvain Brun, pers. comm.) and the nuclei number differences per cell between homokaryons and heterokaryons have not been investigated.

Possible confounding effects

Nuclear losses have been shown to occur within a heterokaryotic mycelium in the *S. tetrasporum* species complex (Vittorelli et al., 2023). However, such a phenomenon, if any effect, would only have attenuated differences between homokaryons and heterokaryons, so that our experiments are conservative regarding this possibility. Furthermore, we found that most heterokaryotic plugs tested had kept nuclei of the two mating types. Even for the mycelia in which we detected a single mating type, it may be that the two mating types are in unbalanced proportions, with the minor one being in frequency beyond the PCR sensitivity threshold (Meunier et al., 2018, Meunier et al., 2022). In addition, large spores have been shown to be sometimes homokaryotic in *S. tetrasporum* (less than 13% of large spores germinated as homokaryons, which may also be due to nucleus loss during growth (Vittorelli et al., 2023)), which might explain the non-significant effect of spore size on germination dynamics.

Conclusions

In conclusion, our findings suggest the presence of a sheltered load, i.e. recessive deleterious mutations at the heterozygous state around the mating-type locus, in three species of Sordariales fungi with young regions of recombination suppression. Leveraging on the experimental assets of fungi, allowing cultivating separately haploid-like and diploid-like life stages, in a system with two mating types permanently heterozygous and genome-wide homozygosity except around the mating-type locus, our experiments provided one of the rare direct experimental evidence of sheltered load around mating-compatibility loci, which is crucial for our understanding of sex-related chromosome evolution.

Competing interests: The authors have no competing interests.

Acknowledgements: This work was supported by the EvolSexChrom ERC advanced grant #832352 (H2020 European Research Council) to T.G. The funders had no role in study design, data collection and analysis, decision to publish, or preparation of the manuscript. We thank Philippe Silar for isolating heterokaryotic strains used here of *Podospora anserina*, *P. comata*, *P. pauciseta*, *Schizothecium tetrasporum* and *S. tritetrasporum* (P. Silar, unpublished), for designing the primer pairs, for the picture of spores in Figure 1 and for advice during the experiment design. We thank Asen Daskalov, Kamalraj Subban and Alexandra Granger-Farbos for isolating MAT1-1 and MAT1-2 homokaryons of the *Podospora anserina*, *P. comata* and *P. pauciseta* strains used in this study. We thank Jacqui Shykoff for discussions on statistical analyses. We thank the collectors of soil and animal faeces: Philippe Silar, Delphine Paumier, Yves Hurand, Pierre Defos du Rau, Jean-Marie Ouary (Milles Traces association), Jérome Letty (Office français de la biodiversité), Paul Jay, Stella McQueen, Karen Vanderwolf, Jacqui Shykoff, Lucas Bonometti and Pierre Gladieux.

534 **Author contribution:** TG, FEH and LG designed experiments. TG obtained funding. LG
535 and EC performed experiments. TG and FEH supervised the study. LG and CL analysed the
536 data. LG produced the figures. TG, FEH and LG wrote the manuscript.

537

References

Ament-Velásquez, S. L. & Vogan, A. A. 2022. Podospora anserina. *Trends in Microbiology* **30**: 1243-1244.

Antonovics, J. & Abrams, J. Y. 2004. Intratetrad mating and the evolution of linkage relationships. *Evolution* **58**: 702-709.

Bachtrog, D. 2005. Sex chromosome evolution: Molecular aspects of Y-chromosome degeneration in Drosophila. *Genome Research* **15**: 1393-1401.

Bachtrog, D. 2013. Y-chromosome evolution : emerging insights into processes of Y-chromosome degeneration. *Nature Reviews Genetics* **14**: 113-124.

Bakkeren, G. & Kronstad, J. W. 1994. Linkage of mating-type loci distinguishes bipolar from tetrapolar mating in basidiomycetous smut fungi. *Proceedings of the National Academy of Sciences of the United States of America* **91**: 7085-7089.

Bergero, R. & Charlesworth, D. 2009. The evolution of restricted recombination in sex chromosomes. *Trends in Ecology & Evolution* **24**: 94-102.

Billiard, S., López-Villavicencio, M., Devier, B., Hood, M., Fairhead, C. & Giraud, T. 2011. Having sex, yes, but with whom? Inferences from fungi on the evolution of anisogamy and mating types. *Biol Rev* **86**: 421-442.

Billiard, S., López-Villavicencio, M., Hood, M. & Giraud, T. 2012. Sex, outcrossing and mating types: unsolved questions in fungi and beyond. *J Evol Biol* **25**: 1020-1038.

Boucher, C., Nguyen, T.-S. & Silar, P. 2017. Species delimitation in the *Podospora anserina, P. pauciseta, P. comata* species complex (Sordariales). *Cryptogamie, Mycologie* **38**: 485-506.

Branco, S., Badouin, H., Rodríguez de la Vega, R. C., Gouzy, J., Carpentier, F., Aguileta, G., Siguenza, S., Brandenburg, J.-T., Coelho, M. A., Hood, M. E. & Giraud, T. 2017. Evolutionary strata on young mating-type chromosomes despite the lack of sexual antagonism. *Proceedings of the National Academy of Sciences* **114**: 7067-7072.

565 Branco, S., Carpentier, F., Rodríguez de la Vega, R. C., Badouin, H., Snirc, A., Le Prieur, S.,
566 Coelho, M. A., de Vienne, D. M., Hartmann, F. E., Begerow, D., Hood, M. E. &
567 Giraud, T. 2018. Multiple convergent supergene evolution events in mating-type
568 chromosomes. *Nature Communications* **9**: 2000.
569 Carpentier, F., de la Vega, R. R. C., Jay, P., Duhamel, M., Shykoff, J. A., Perlin, M. H.,
570 Wallen, R. M., Hood, M. E. & Giraud, T. 2022. Tempo of degeneration across
571 independently evolved nonrecombining regions. *Molecular Biology and Evolution* **39**.
572 Charlesworth, B. & Charlesworth, D. 2000. The degeneration of Y chromosomes.
573 *Philosophical Transactions of the Royal Society B-Biological Sciences* **355**: 1563-
574 1572.
575 Charlesworth, D. 2017. Evolution of recombination rates between sex chromosomes.
576 *Philosophical Transactions of the Royal Society B-Biological Sciences* **372**.
577 Colegrave, N. 2002. Sex releases the speed limit on evolution. *Nature* **420**: 664-666.
578 Contamine, V., Zickler, D. & Picard, M. 2004. The *Podospora* rmp1 gene implicated in
579 nucleus-mitochondria cross-talk encodes an essential protein whose subcellular
580 location is developmentally regulated. *Genetics* **166**: 135-150.
581 Duhamel, M., Hood, M. E., Rodriguez de la Vega, R. C. & Giraud, T. 2023. Dynamics of
582 transposable element accumulation in the non-recombining regions of mating-type
583 chromosomes in anther-smut fungi. *Nature Communications* **14**: 5692
584 Felsenstein, J. 1974. The evolutionary advantage of recombination. *Genetics* **78**: 737-756.
585 Fisher, R. A. 1930. *The genetical theory of natural selection*.
586 Fontanillas, E., Hood, M. E., Badouin, H., Petit, E., Barbe, V., Gouzy, J., De Vienne, D. M.,
587 Aguileta, G., Poulain, J., Wincker, P., Chen, Z., Toh, S. S., Cuomo, C. A., Perlin, M.
588 H., Gladieux, P. & Giraud, T. 2015. Degeneration of the nonrecombining regions in
589 the mating-type chromosomes of the anther-smut fungi. *Molecular Biology and*
590 *Evolution* **32**: 928-943.

591 Fraser, J. A., Diezmann, S., Subaran, R. L., Allen, A., Lengeler, K. B., Dietrich, F. S. &
592 Heitman, J. 2004. Convergent evolution of chromosomal sex-determining regions in
593 the animal and fungal kingdoms. *Plos Biol.* **2**: 2243-2255.
594 Gemmell, N. J. & Slate, J. 2006. Heterozygote advantage for fecundity. *PLoS One* **1**: e125.
595 Giraud, T., Yockteng, R., Lopez-Villavicencio, M., Refregier, G. & Hood, M. E. 2008. The
596 mating system of the anther smut fungus, *Microbotryum violaceum*: selfing under
597 heterothallism. *Euk. Cell* **7**: 765-775.
598 Glémin, S., Bataillon, T., Ronfort, J., Mignot, A. & Olivieri, I. 2001. Inbreeding depression in
599 small populations of self-incompatible plants. *Genetics* **159**: 1217-29.
600 Goubet, P. M., Bergès, H., Bellec, A., Prat, E., Helmstetter, N., Mangenot, S., Gallina, S.,
601 Holl, A.-C., Fobis-Loisy, I., Vekemans, X. & Castric, V. 2012. Contrasted Patterns of
602 Molecular Evolution in Dominant and Recessive Self-Incompatibility Haplotypes in
603 Arabidopsis. *PLOS Genetics* **8**: e1002495.
604 Grognet, P., Bidard, F., Kuchly, C., Tong, L. C. H., Coppin, E., Benkhali, J. A., Couloux, A.,
605 Wincker, P., Debuchy, R. & Silar, P. 2014. Maintaining two mating types: structure of
606 the mating type locus and its role in heterokaryosis in *Podospora anserina*. *Genetics*
607 **197**: 421-432.
608 Hallast, P., Ebert, P., Loftus, M., Yilmaz, F., Audano, P. A., Logsdon, G. A., Bonder, M. J.,
609 Zhou, W., Höps, W., Kim, K., Li, C., Hoyt, S. J., Dishuck, P. C., Porubsky, D.,
610 Tsetsos, F., Kwon, J. Y., Zhu, Q., Munson, K. M., Hasenfeld, P., Harvey, W. T.,
611 Lewis, A. P., Kordosky, J., Hoekzema, K., O'Neill, R. J., Korbel, J. O., Tyler-Smith,
612 C., Eichler, E. E., Shi, X., Beck, C. R., Marschall, T., Konkel, M. K., Lee, C. & Human
613 Genome Structural Variation, C. 2023. Assembly of 43 human Y chromosomes
614 reveals extensive complexity and variation. *Nature* **621**: 355-364.
615 Hartmann, F. E., Ament-Velasquez, S. L., Vogan, A. A., Gautier, V., Le Prieur, S.,
616 Berramdane, M., Snirc, A., Johannesson, H., Grognet, P., Malagnac, F., Silar, P. &
617 Giraud, T. 2021a. Size variation of the nonrecombining region on the mating-type

chromosomes in the fungal *Podospora anserina* species complex. *Molecular Biology and Evolution* **38**: 2475-2492.

Hartmann, F. E., Duhamel, M., Carpentier, F., Hood, M. E., Foulongne-Oriol, M., Silar, P., Malagnac, F., Grognet, P. & Giraud, T. 2021b. Recombination suppression and evolutionary strata around mating-type loci in fungi: documenting patterns and understanding evolutionary and mechanistic causes. *New Phytologist* **229**: 2470-2491.

Hill, J., Enbody, E. D., Bi, H., Lamichhaney, S., Lei, W., Chen, J., Wei, C., Liu, Y., Schwochow, D., Younis, S., Widemo, F. & Andersson, L. 2023. Low mutation load in a supergene underpinning alternative male mating strategies in Ruff *(Calidris pugnax)*. **40**.

Hill, W. G. & Robertson, A. 1966. The effect of linkage on limits to artificial selection. *Genetics Research* **8**: 269-294.

Hood, M. E. & Antonovics, J. 2000. Intratetrad mating, heterozygosity, and the maintenance of deleterious alleles in *Microbotryum violaceum (= Ustilago violacea)*. *Heredity* **85**: 231-241.

Hough, J., Hollister, J. D., Wang, W., Barrett, S. C. H. & Wright, S. I. 2014. Genetic degeneration of old and young y chromosomes in the flowering plant *Rumex hastatulus*. *Proceedings of the National Academy of Sciences of the United States of America* **111**: 7713-7718.

Jay, P., Chouteau, M., Whibley, A., Bastide, H., Parrinello, H., Llaurens, V. & Joron, M. 2021. Mutation load at a mimicry supergene sheds new light on the evolution of inversion polymorphisms. *Nature Genetics* **53**: 288-293.

Jay, P., Jeffries, D., Hartmann, F. E., Véber, A. & Giraud, T. 2024. Why do sex chromosomes progressively lose recombination? *Trends in Genetics* **40**: 564-579.

Jay, P., Tezenas, E., Véber, A. & Giraud, T. 2022. Sheltering of deleterious mutations explains the stepwise extension of recombination suppression on sex chromosomes and other supergenes. *PLoS Biology* **20**: e3001698.

646 Judelson, H. S., Spielman, L. J. & Shattock, R. C. 1995. Genetic mapping and non-
647 Mendelian segregation of mating type loci in the oomycete, Phytophthora infestans.
648 *Genetics* **141**: 503-12.
649 Lenormand, T. & Roze, D. 2022. Y recombination arrest and degeneration in the absence of
650 sexual dimorphism. *Science* **375**: 663-+.
651 Llaurens, V., Gonthier, L. & Billiard, S. 2009. The sheltered genetic load linked to the S locus
652 in plants: new insights from theoretical and empirical approaches in sporophytic self-
653 incompatibility. *Genetics* **183**: 1105-1118.
654 Ma, W.-J. & Veltsos, P. 2021. The diversity and evolution of sex chromosomes in frogs.
655 *Genes* **12**: 483.
656 Mena-Alí, J. I., Keser, L. H. & Stephenson, A. G. 2009. The effect of sheltered load on
657 reproduction in Solanum carolinense, a species with variable self-incompatibility. *Sex*
658 *Plant Reprod* **22**: 63-71.
659 Menkis, A., Jacobson, D. J., Gustafsson, T. & Johannesson, H. 2008. The mating-type
660 chromosome in the filamentous ascomycete *Neurospora tetrasperma* represents a
661 model for early evolution of sex chromosomes. *PLoS Genet.* **4**: e1000030.
662 Meunier, C., Darolti, I., Reimegård, J., Mank, J. E. & Johannesson, H. 2022. Nuclear-specific
663 gene expression in heterokaryons of the filamentous ascomycete Neurospora
664 tetrasperma. *Proc Biol Sci* **289**: 20220971.
665 Meunier, C., Hosseini, S., Heidari, N., Maryush, Z. & Johannesson, H. 2018. Multilevel
666 selection in the filamentous ascomycete *Neurospora tetrasperma*. *The American*
667 *Naturalist* **191**: 290-305.
668 Muller, H. J. 1932. Some genetic aspects of sex. *The American Naturalist* **66**: 118-138.
669 Nicolas, M., Marais, G. A. B., Hykelova, V., Janousek, B., Laporte, V., Vyskot, B.,
670 Mouchiroud, D., Negrutiu, I., Charlesworth, D. & Monéger, F. 2004. A gradual
671 process of recombination restriction in the evolutionary history of the sex
672 chromosomes in dioecious plants. *PLoS Biology* **3**: e4.
673 Otto, S. P. 2009. The evolutionary enigma of sex. *Am. Nat.* **174**: S1-S14.

674 Oudemans, P. V., Alexander, H. M., Antonovics, J., Altizer, S., Thrall, P. H. & Rose, L. 1998.
675 The distribution of mating-type bias in natural populations of the anther-smut Ustilago
676 violacea on *Silene alba* in Virginia. *Mycologia* **90**: 372-381.
677 Papadopulos, A. S. T., Chester, M., Ridout, K. & Filatov, D. A. 2015. Rapid Y degeneration
678 and dosage compensation in plant sex chromosomes. *Proceedings of the National*
679 *Academy of Sciences* **112**: 201508454.
680 R Core Team 2023. R: A Language and Environment for Statistical Computing. . *R*
681 *Foundation for Statistical Computing, Vienna, Austria*.
682 Raju, N. B. & Perkins, D. D. 1994. Diverse programs of ascus development in
683 pseudohomothallic species of Neurospora, Gelasinospora, and Podospora.
684 *Developmental Genetics* **15**: 104-118.
685 Rice, W. R. & Chippindale, A. K. 2001. Sexual recombination and the power of natural
686 selection. *Science* **294**: 555-559.
687 Schneider, C. A., Rasband, W. S. & Eliceiri, K. W. 2012. NIH Image to ImageJ: 25 years of
688 image analysis. *Nature Methods* **9**: 671-675.
689 Schwander, T., Libbrecht, R. & Keller, L. 2014. Supergenes and complex phenotypes.
690 *Current Biology* **24**: R288-R294.
691 Shen, L., Chapeland-Leclerc, F., Ruprich-Robert, G., Chen, Q., Chen, S., Adnan, M., Wang,
692 J., Liu, G. & Xie, N. 2022. Involvement of VIVID in white light-responsive
693 pigmentation, sexual development and sterigmatocystin biosynthesis in the
694 filamentous fungus Podospora anserina. *Environ Microbiol* **24**: 2907-2923.
695 Silar, P. 2020. *Podospora anserina*. hal-02475488.
696 Smith, J. M. & Haigh, J. 2009. The hitch-hiking effect of a favourable gene. *Genetical*
697 *Research* **23**: 23-35.
698 Stone, J. 2004. Sheltered load associated with S-alleles in Solanum carolinense. *Heredity*
699 **92**: 335-342.

Tezenas, E., Giraud, T., Véber, A. & Billiard, S. 2023. The fate of recessive deleterious or overdominant mutations near mating-type loci under partial selfing. *Peer Community Journal* **3**: e14.

Thomas, A., Shykoff, J., Jonot, O. & Giraud, T. 2003. Sex-ratio bias in populations of the phytopathogenic fungus *Microbotryum violaceum* from several host species. *International Journal of Plant Sciences* **164**: 641-647.

Uyenoyama, M. K. 2005. Evolution under tight linkage to mating type. *New Phytologist* **165**: 63-70.

Vittorelli, N., Rodríguez de la Vega, R. C., Snirc, A., Levert, E., Gautier, V., Lalanne, C., De Filippo, E., Gladieux, P., Guillou, S., Zhang, Y., Tejomurthula, S., Grigoriev, I. V., Debuchy, R., Silar, P., Giraud, T. & Hartmann, F. E. 2023. Stepwise recombination suppression around the mating-type locus in an ascomycete fungus with self-fertile spores. *PLoS Genetics* **19**: e1010347.

Whittle, C. A., Sun, Y. & Johannesson, H. 2011. Degeneration in codon usage within the region of suppressed recombination in the mating-type chromosomes of *Neurospora tetrasperma*. *Eukaryotic Cell* **10**: 594-603.

Wielstra, B. 2020. Balanced lethal systems. *Current Biology* **30**: R742-R743.

Wright, A. E., Dean, R., Zimmer, F. & Mank, J. E. 2016. How to make a sex chromosome. *Nature Communications* **7**: 12087.

Zakharov, I. A. 2005. [Intratetrad mating and its genetic and evolutionary consequences]. *Genetika* **41**: 508-19.

Zakharov, I. A. 2023. Intratetrad mating as the driving force behind the formation of sex chromosomes in fungi. *Trends in Genetics and Evolution* **6**: doi: 10.24294/tge.v6i1.252.

727

728 **Table 1:** Number of strains from *Schizothecium tetrasporum, Schizothecium tritetrasporum,*
729 *Podospora anserina, Podospora comata* and *Podospora pauciseta* used for experiments,
730 summary of the conditions (light and temperature) and measure time points for which fitness
731 proxies (growth speed or germination dynamics) were assessed according to species and
732 strains. Information on strains can be found in Table S1.

Growth speed				
Species	**Number of strains**	**Measure time points (days)**	**Temperature**	**Light exposure**
S. tetrasporum	10	6 / 14	22°C	Yes
S. tetrasporum	10	6 / 14	22°C	No
S. tritetrasporum	13	6 / 14	22°C	Yes
P. anserina	17	2 / 6	18°C	Yes
P. anserina	17	2 / 6	37°C	Yes
P. comata	1	2 / 6	18°C	Yes
P. comata	1	2 / 6	37°C	Yes
P. pauciseta	3	2 / 6	18°C	Yes
P. pauciseta	3	2 / 6	37°C	Yes

Germination dynamics		
Species	**Number of strains**	**Measurement time points (days)**
S. tetrasporum	8	2 / 3 / 7

733

734

Figures

Figure 1: Fitness experiments to test for the presence of a sheltered load in pseudo-homothallic ascomycete fungi, i.e. producing heterokaryotic spores (with nuclei of the two mating types), and with therefore a main phase of the life cycle being heterokaryotic. A) Schema illustrating how the life cycle of pseudo-homothallic fungi can be used to test for the existence of sheltered load (i.e the presence of heterozygous recessive deleterious mutations) in the non-recombining region around mating-type loci. **B)** Pictures of mycelium after six days of growth on Petri dishes under light conditions at 22°C, with heterokaryons at left, *MAT1-2* homokaryons in the middle and *MAT1-1* homokaryons at right, for *Schizothecium tritetrasporum* (strain PSN935D), *Schizothecium tetrasporum* (strain PSN781A) and *Podospora anserina* (strain Wa68), from top to bottom. Scale bar: 4 cm. **C)** Picture of *Schizothecium tetrasporum* spores (strain CBS815.71), with two small on *the* top right and two large on *the* bottom left. The large spores have length and width of ca. 25 x 12 µm.

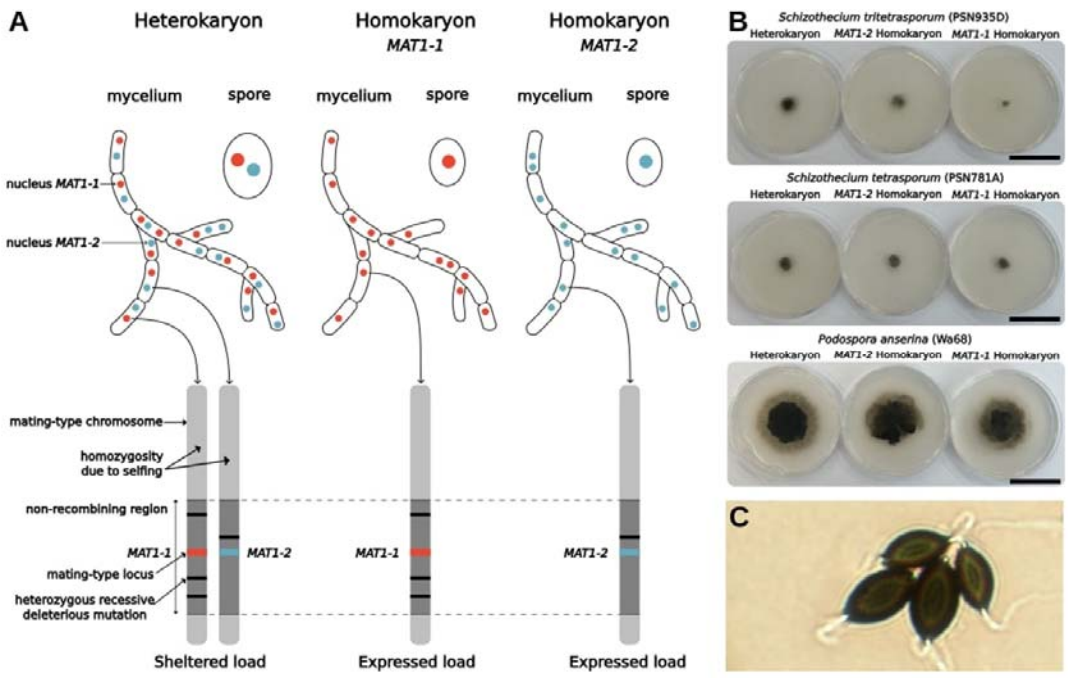

Figure 2: Mycelium growth speed of heterokaryons versus homokaryons in *Schizothecium tritetrasporum*. Mycelium growth speed (mm.day^{-1}) of heterokaryons (in purple), *MAT1-1* homokaryons (in red) and *MAT1-2* homokaryons (in blue), between day 6 and day 14 estimated from two batches of three replicates using 12 strains grown under light conditions at 22°C. Dots and bars represent estimated means and standard deviations from a linear mixed-effect model explaining growth speed using the nuclear status (*MAT1-1* homokaryon, *MAT1-2* homokaryon or heterokaryon) as fixed effect and strain ID and batch as random effects. P-values correspond to t-tests with Satterthwaite correction (ns: non significant; *** = p<0.001).

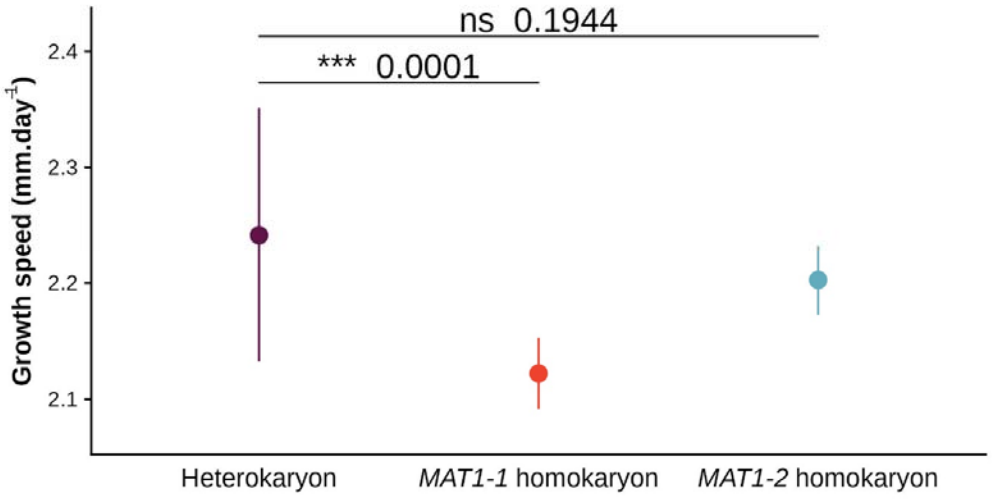

Figure 3: Mycelium growth speed of heterokaryons versus homokaryons in *Schizothecium tetrasporum*, under light and dark conditions. Mycelium growth speed (mm.day^{-1}) of heterokaryons (in purple), *MAT1-1* homokaryons (in red) and *MAT1-2* homokaryons (in blue), between day 6 and day 14 estimated from three replicates using 10 strains grown under **A)** light or **B)** dark conditions, both at 22°C. Dots and bars represent estimated means and standard deviations from a linear mixed-effect model explaining growth speed using the nuclear status (*MAT1-1* homokaryon, *MAT1-2* homokaryon or heterokaryon) as a fixed effect and strain ID as a random effect. P-values correspond to t-tests with Satterthwaite correction (ns: non significant; * = p<0.05).

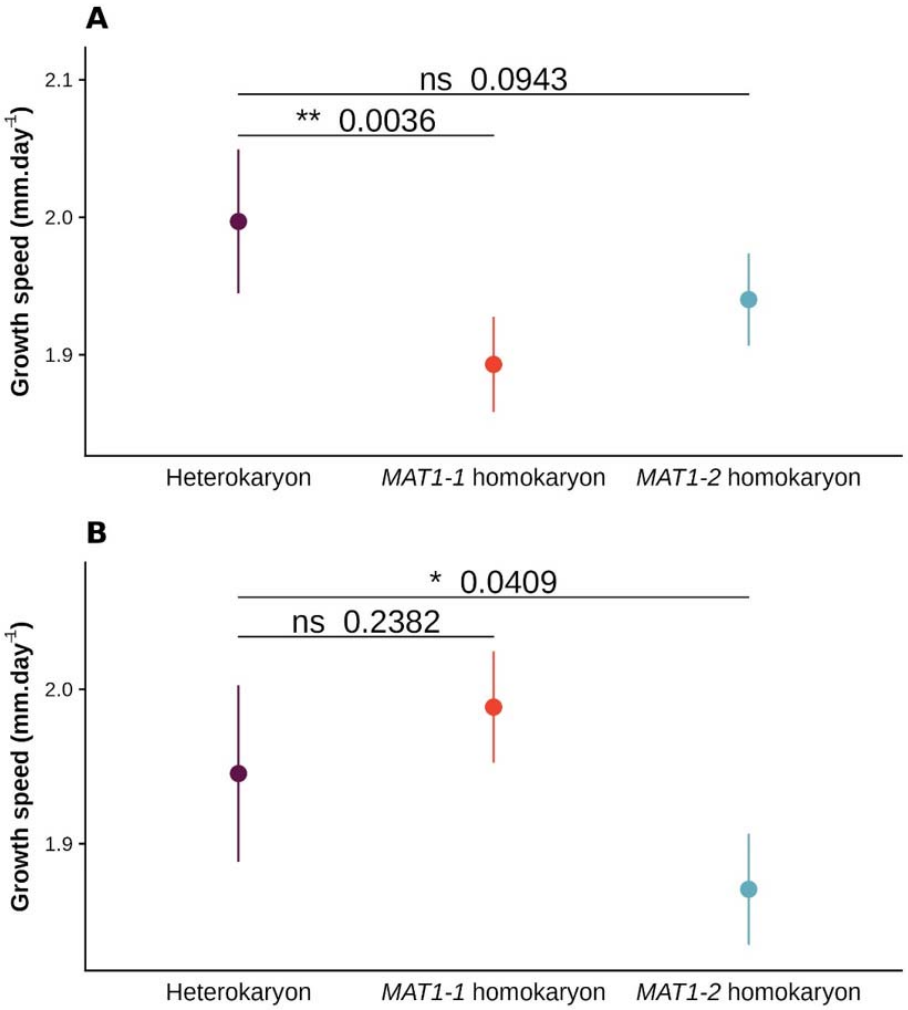

Figure 4: Mycelium growth speed of heterokaryons versus homokaryons in *Podospora anserina*, under two different temperatures. Mycelium growth speed (mm.day^{-1}) of heterokaryons (in purple), *MAT1-1* homokaryons (in red) and *MAT1-2* homokaryons (in blue), between day 2 and day 6 estimated from three replicates using 17 strains grown at **A**) 18°C or **B**) 37°C, both under light conditions. Dots and bars represent estimated means and standard deviations using a linear mixed-effect model explaining growth speed using the nuclear status (*MAT1-1* homokaryon, *MAT1-2* homokaryon or heterokaryon) as a fixed effect and strain ID as a random effect. P-values correspond to t-tests with Satterthwaite correction (ns: non significant; ** = p<0.01).

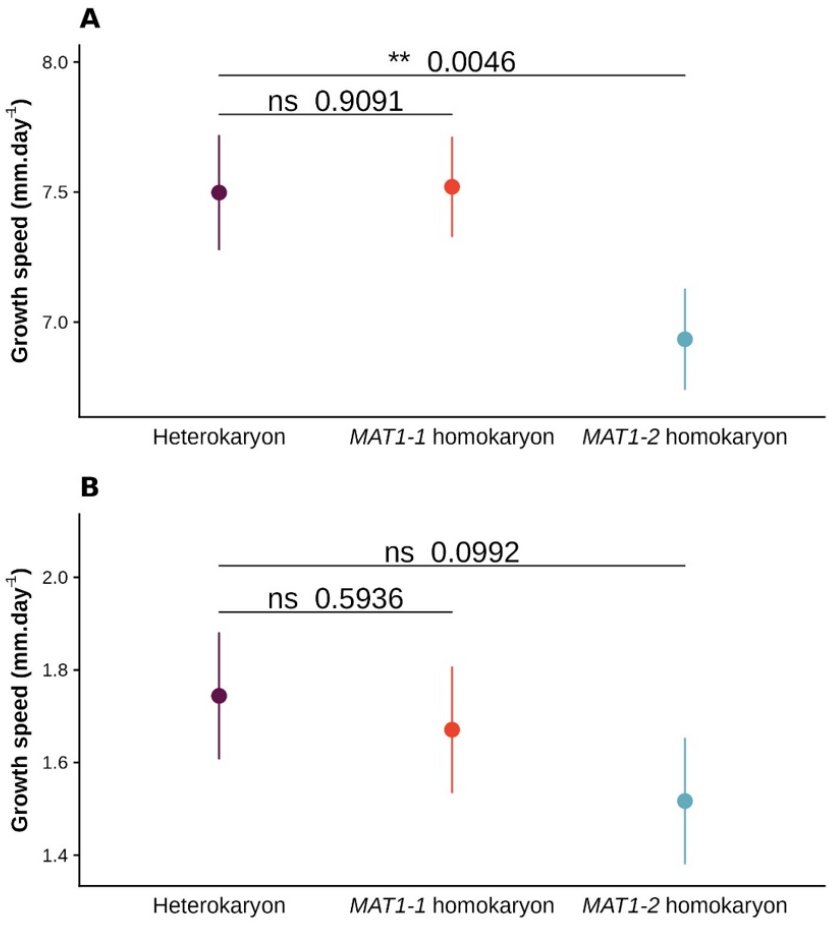

Figure 5: Mycelium growth speed of heterokaryons versus homokaryons in *Podospora pauciseta* and *Podospora comata*, under two different temperatures. Mycelium growth speed (mm.day^{-1}) of heterokaryons (in purple), *MAT1-1* homokaryons (in red) and *MAT1-2* homokaryons (in blue), between day 2 and day 6 estimated from 3 replicates using three strains for *P. pauciseta* (**A** and **B**) and a single strain for *P. comata* (**C** and **D**) grown at 18°C (**A** and **C**) or 37°C (**B** and **D**) under light conditions. Dots and bars represent estimated means and standard deviations from a linear mixed-effect model for *P. pauciseta* or a linear model for *P. comata* explaining the growth speed using the nuclear status (*MAT1-1* homokaryon, *MAT1-2* homokaryon or heterokaryon) as a fixed effect and strain ID as a random effect for *P. pauciseta*. P-values correspond to t-tests (with Satterthwaite correction for the mixed-effect models) (ns: not significant; * = p<0.05).

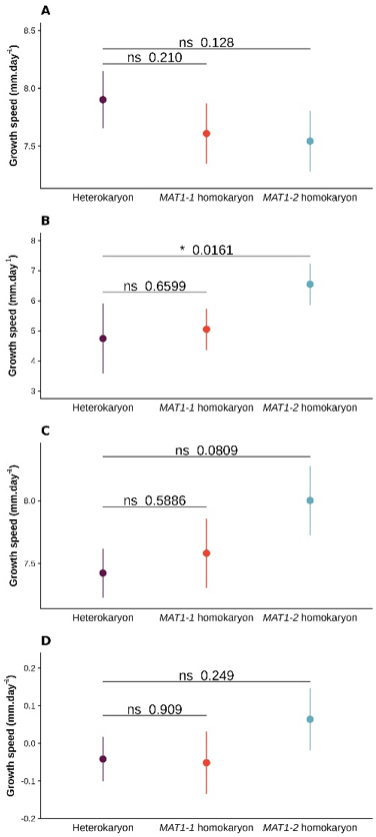

Figure 6: Spore germination dynamics in *Schizothecium tetrasporum*, depending on their heterokaryotic versus homokaryotic nuclear status. Germination rate dynamics for small spores (in purple) and large spores (in grey) estimated from eight strains from germination rates on day 2, day 3 and day 7 from two batches of 10 spores per strain and per spore size class. The fit of the germination dynamics was done by maximum likelihood with Laplace approximation using a generalised linear mixed-effect model with a Binomial distribution modelling germination rate as a linear combination of day (as a continuous predictor) and spore size class (large or small) treated as fixed effects and strain ID and batch as random effects. P-values correspond to $\chi 2$-tests (spore size effect: p=0.4459; day effect: p= 0.0178).

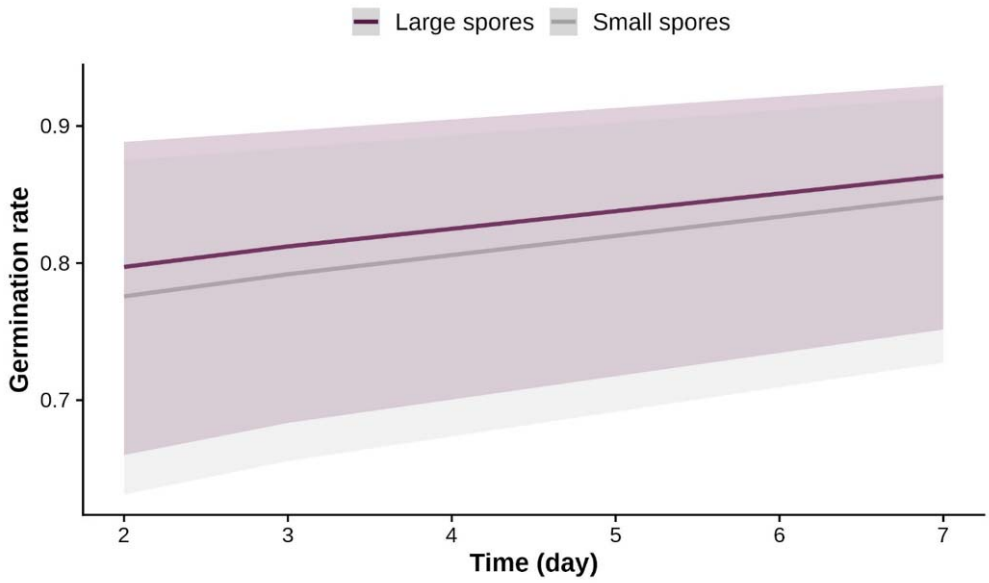

Supplementary Figures

Supplementary Figure S1: Mycelium growth speed of heterokaryons versus homokaryons for 13 strains of *Schizothecium tritetrasporum*. Mycelium growth speed (mm.day^{-1}) of heterokaryons (in purple), *MAT1-1* homokaryons (in red) and *MAT1-2* homokaryons (in blue), of the three replicates for each of two batches, for the 13 strains of *S. tritetrasporum*, between day 6 and day 14 grown under light conditions at 22°C. Green dots highlight the heterokaryon replicates for which less than 50% of the nine mycelium plugs from the Petri dish were genotyped heterokaryotic. Boxplot elements: central line: median, box limits: 25th and 75th percentiles, whiskers: 1.5× interquartile range.

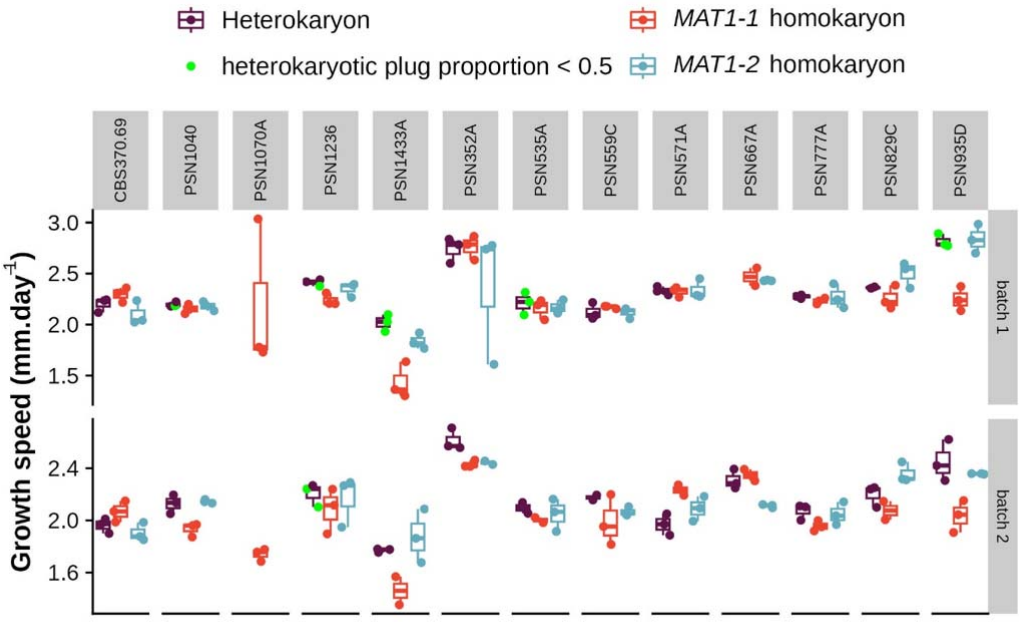

833 **Supplementary Figure S2: Mycelium growth speed of heterokaryons versus**

834 **homokaryons for 10 strains of *Schizothecium tetrasporum*.** Mycelium growth speed

835 (mm.day^{-1}) of heterokaryons (in purple), *MAT1-1* homokaryons (in red) and *MAT1-2*

836 homokaryons (in blue), of the three replicates of the 10 strains of *S. tetrasporum* between day

837 6 and day 14 grown under **A**) light or **B**) dark conditions at 22°C. Boxplot elements: central

838 line: median, box limits: 25th and 75th percentiles, whiskers: 1.5× interquartile range.

839

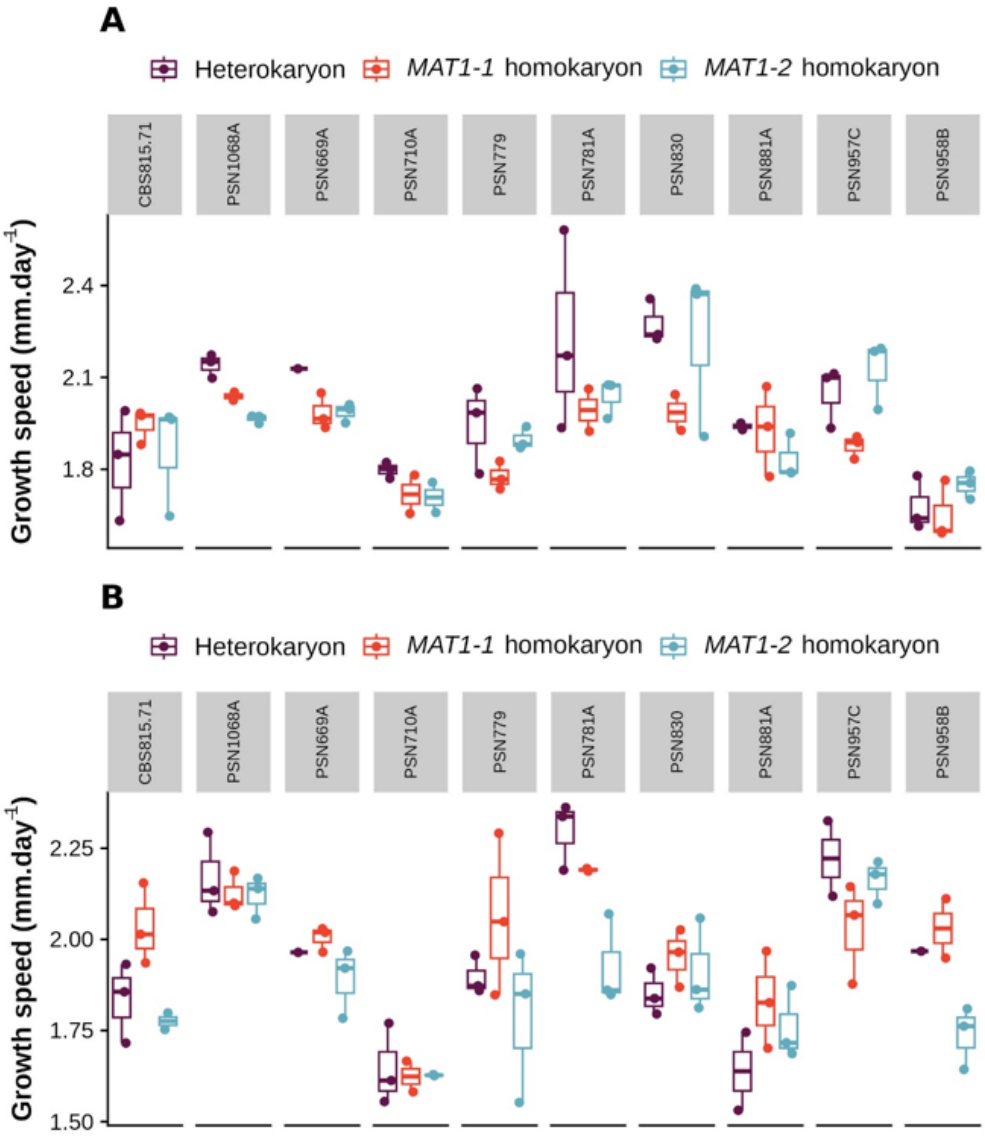

840

841

842

843 **Supplementary Figure S3: Estimates of nuclear loss in *Schizothecium tritetrasporum***

844 **mycelium.** Proportion of heterokaryotic plugs (i.e. with both *MAT1-1* and *MAT1-2* alleles

845 detected by PCR) in *S. tritetrasporum* mycelium after 14 days of growth. Proportions were

846 calculated out of nine plugs per plate in three replicates per strain in two batches that were

847 genotyped by PCR.

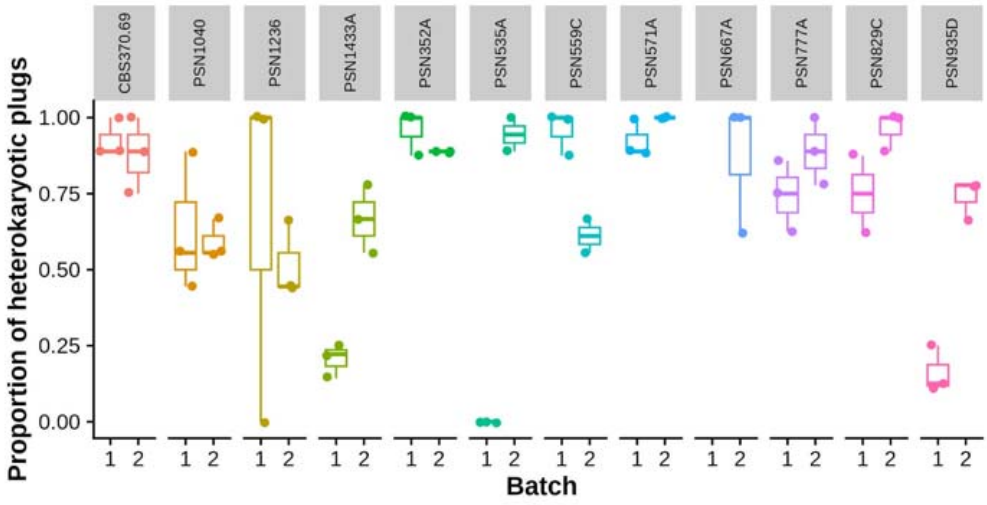

848

849

850

851

852

853

854

855

856

Supplementary Figure S4: Mycelium growth speed of heterokaryons versus homokaryons for 17 strains of *Podospora anserina*. Mycelium growth speed (mm.day^{-1}) of heterokaryons (in purple), *MAT1-1* homokaryons (in red) and *MAT1-2* homokaryons (in blue), of the three replicates of the 17 strains of *P. anserina* between day 2 and day 6 grown at **A**) 18°C or **B**) 37°C under light conditions. Boxplot elements: central line: median, box limits: 25th and 75th percentiles, whiskers: 1.5× interquartile range.

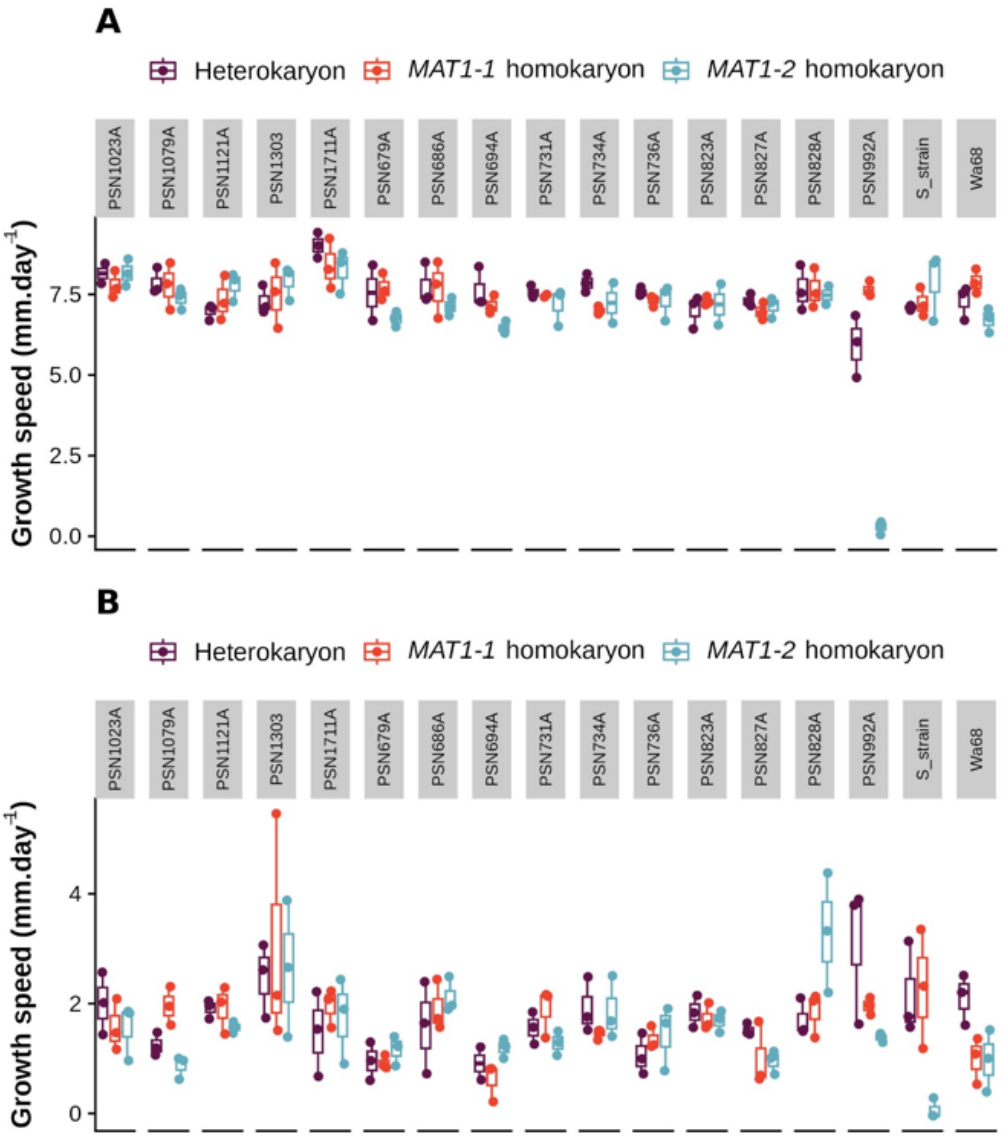

Supplementary Figure S5: Mycelium growth speed of heterokaryons versus homokaryons for one strain of *Podospora comata* and three strains of *Podospora pauciseta*. Mycelium growth speed (mm.day^{-1}) of heterokaryons (in purple), *MAT1-1* homokaryons (in red) and *MAT1-2* homokaryons (in blue), of the three replicates of the three strains for *P. pauciseta* (**A** and **B**) and the single strain for *P. comata* (**C** and **D**) between day 2 and day 6 grown at 18°C (**A** and **C**) or 37°C (**B** and **D**) under light conditions. Boxplot elements: central line: median, box limits: 25th and 75th percentiles, whiskers: 1.5× interquartile range.

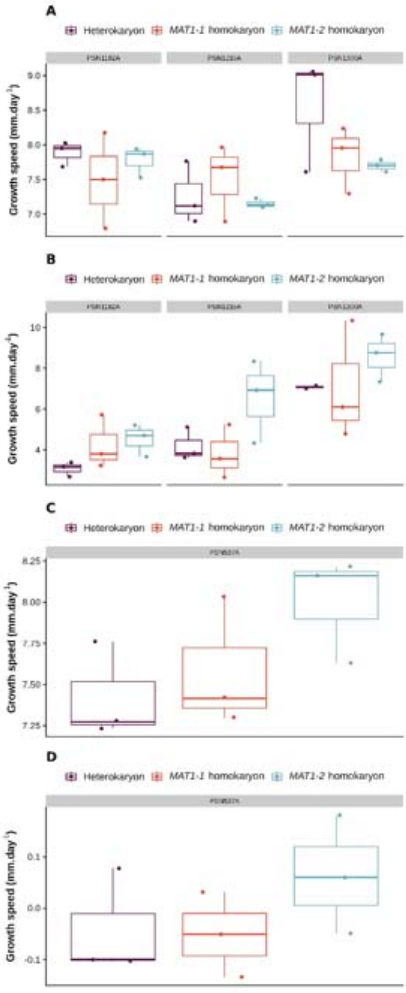

875 **Supplementary Figure S6: Spore germination rate for eight strains of *Schizothecium***
876 ***tritetrasporum*, depending on their heterokaryotic versus homokaryotic nuclear status.**
877 Germination rate on days 2, 3 and 7 for small spores and large spores of the 10 spores of the
878 two batches of the eight strains of *S. tetrasporum*. Symbol shapes correspond to batches.
879 Boxplot elements: central line: median, box limits: 25th and 75th percentiles, whiskers: 1.5×
880 interquartile range.
881

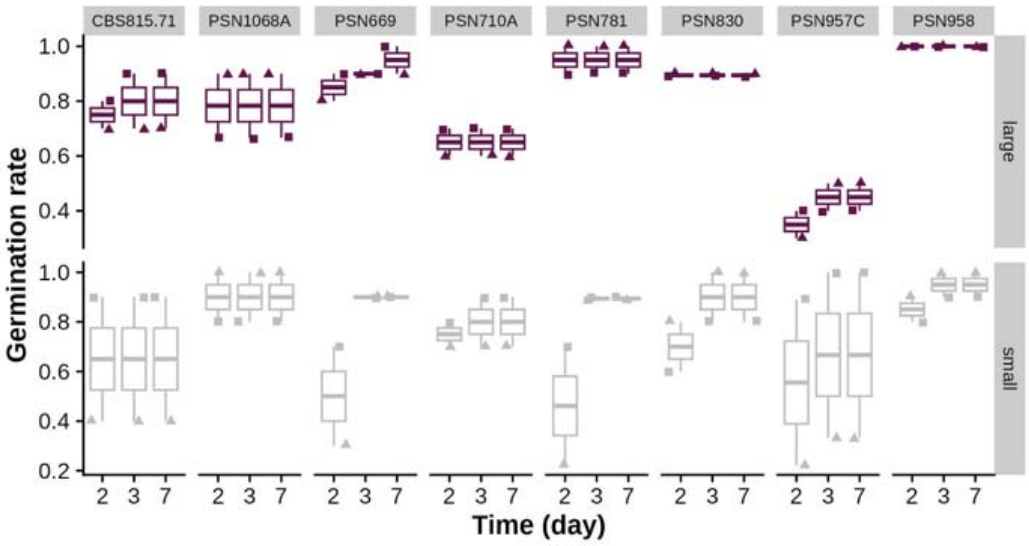

882
883
884